Check for updates

Original Article

JOURNAL OF TEXTILES AND FIBROUS MATERIALS

Journal of Textiles and Fibrous Materials
Volume 1: 1–13
© The Author(s) 2018
DOI: 10.1177/2515221118788370
journals.sagepub.com/home/tex
SAGE

Chitosan nanofibrous materials for chemical and biological protection

Mukesh Kumar Sinha[1] and Biswa Ranjan Das[1]

Abstract

Chitosan derivatives are difficult to electrospun because they have poor flexibility of their polyelectrolyte chains. Based on extensive trails, we have successfully electrospun chitosan polymer and, subsequently, coated on non-woven polypropylene utilizing Nanospider technology. This experimentally developed nanofibrous webs of various densities were coated on non-woven fabric and, subsequently, stitched with activated carbon sphere (ACS) adhered composite fabric. Biological filtration and chemical protection were evaluated and the optimized density offering the highest value with meeting specified comfort was assessed. Results showed that optimized web morphology of 0.43 g m^{-2} is the best for integration with nuclear, biological and chemical absorbent layer of low ACS add-on in all aspects of comfort and protective behaviours. This will be meeting stringent defence protective requirements and lowering down the weight of suit by approximately 25%. An attempt has also been made in this research to protect from sulphur mustard chemical warfare agent by using both theories: (a) barrier techniques and (b) disintegrating the trapped molecules via functionalization of the web. Result shows that first molecules get trapped by in web layer (barrier effect) and subsequently destroyed by hydrolysis mechanism. Scanning microscopic image shows web is acting as barrier layer by trapping sulphur mustard particles. Optimized web of 0.43 g m^{-2} was functionalized with zinc (Zn) oxide and the presence of Zn particles was confirmed by imaging techniques. Crystalline and thermal analysis depicts that structural changes were found in sulphur mustard spotted functionalized web. Raman spectra show chemically disintegrated hydrolysed products of sulphur mustard. Bacterial filtration efficiency, antimicrobial and comfort properties were measured for assessing the introduction of nanowebs for biological protection and chemical protection in newly created multilayered fabric structure with low ACS add-on (180 g m^{-2}). The initial encouraging outcome of this research expects whether the multilayered fabric could be introduced in the suit.

Keywords

Antimicrobial, biological, chemical, chitosan, morphology, nanowebs

Date received: 24 May 2018; Received revised June 12, 2018; accepted: 18 June 2018

Introduction

Advancements in nanotechnology are revolutionizing our capability to understand its applications in many thrust research areas of technical textiles and materials science. Nanofibrous materials are believed to play a pivotal role in engineering of many materials to be used individually or integrated with the other substrate to introduce various functional features at a very low mass density. These potential materials are recent addition to textiles for developing breathable protective fabrics offering biological and chemical protection and are developed successfully and economically by the electrospinning process.

[1] Defence Materials and Stores and Research and Development Establishment, Defence Research and Development Organization, Uttar Pradesh, India

Corresponding author:
Mukesh Kumar Sinha, Defence Materials and Stores and Research and Development Establishment, Defence Research and Development Organization (DRDO), Ministry of Defence, Government of India, G. T. Road, Kanpur-208013, Uttar Pradesh, India.
Email: muk120in@yahoo.co.in

Creative Commons CC BY: This article is distributed under the terms of the Creative Commons Attribution 4.0 License (http://www.creativecommons.org/licenses/by/4.0/) which permits any use, reproduction and distribution of the work without further permission provided the original work is attributed as specified on the SAGE and Open Access pages (https://us.sagepub.com/en-us/nam/open-access-at-sage).

Protective fabrics are described as garments for functional performance and characteristics, rather than their designs or decorative purposes. Out of which defence protective fabric specifications are highly stringent and demanding with respect to functional protective performance. Currently, military personnel need to be safeguarded against all kinds of man-made and climatic threats by providing lower weight apparels with enhanced comfort. Defence protective textile (DPT; clothing) is categorized as stealth and camouflage; nuclear, biological and chemical (NBC); extreme cold weather and ballistic and so on.[1–3]

The unique properties of nanofibres such as high-specific surface area, inter-connected pore structure, surface functionality and high porosity create a new value for the traditional textiles and fabrics and have been integrated into a wide range of applications including various segments of air filtration, liquid filtration, wound dressing, tissue scaffolds, waterproof and breathable membranes and defence protective fabrics.[4–9] That are the reason, emerging nano textile technology can play a vital role to meet such stringent functional demand for military personnel. Still, this technology is mostly used for biomedical applications, for example, wound healing, drug delivery, tissue engineering and bone healing. Producing webs are of practical use and can have integrated with textile fabric structure or alone it could be used as functional protective layer for example, chemical, biological, virus, flame retardant, antimicrobial and bacterial filtration. The most challenging task is to prepare nanofibre webs with adequate durability, structural integrity (due to high abrasion and flexing action) and fastness to laundering and washing.

Out of all types of DPTs, NBC is most dangerous and important for future war scenario. NBC suit is used as protective permeable and disposable combat apparel intended to be used in chemical warfare agents (CWAs) contaminated environment. The currently existing item protects against CWAs followed by very limited protection against biological agents. Materials used in this require continuous improvements to keep pace with state-of-the-art protective technology. The most vital feature currently required to be introduced in this product is biological protection with enhanced chemical adsorption and lighter weight. Activated carbon sphere (ACS) adhered composite fabric is the most important component of NBC suit for offering chemical protection. The existing ACS adhered composite fabric used in NBC suit is having mass of approximately 400–410 g m^{-2} and offering dichloropropane (DCP) penetration rate of 180 s and chemical protection of 24 h. Hence, attempt is made in stitching of nanofibrous webs along with this component to enhance its chemical adsorption and biological filtration at reduced weight. For this reason, production process of chitosan nanofibrous webs was explored. Chitosan is obtained after deacetylation of natural chitin sources and this material is inherently, biopolymer, antimicrobial and biodegradable.[10–13] However, it is difficult to electrospin chitosan due to its higher polarity and non-flexibility of chain. Till date, this material was not utilized for making DPTs. In this research work, such critical materials were electrospun and these nanowebs's morphology has been studied against defence protective functional behaviours. Morphology of nanofibre is also an important property for deciding comfort of fabrics.[14] Thus, such scientific approach and studies are application-oriented research work for defence protective functional textiles.

Experimental

Sample preparation. Chitosan (molecular weight approximately 90,000 g mol^{-1} and Degree of deacetylation (DDA) approximately 75%) of Aldrich Company, Sigma–Aldrich Company Ltd, Gillingham, UK was dissolved by magnetic stirring in trifluroacetic acid and dichloromethane (2:8 ratios) for 18 h at 50°C. Antistat polypropylene (PP) spunbonded (approximately 30 g m^{-2}) non-woven fabric having surface resistivity in the order of approximately 10^{10} Ω·cm was used as a coating substrate. The prepared solution was electrospun through Nanospider machine (NS LAB 200 series version 1.1) for fabricating PP-coated webs with vigorous experimental trials. The best optimal condition was found for spinning: 13% Chitosan was successfully electrospun (superlative web structure) in the electric field of 65 kV, distance between spinning electrodes 135 mm and rotation of drum spinning electrode 8 r min^{-1} (throughput). Similar process was repeated with varying collector speed and maintaining other parameters constant, for obtaining different webs from denser (thicker) to thinner morphology. The best optimal condition was used to fabricate webs with different coating speed varied from 0.18 m min^{-1} to 1.15 m min^{-1}. Air drying of web was carried out for 30 min to remove residual water molecules. Out of these fabricated nanowebs of different structures, best optimized web in terms of properties like comfort, air permeability and water vapour transportation properties was taken further for functionalization by zinc oxide (ZnO) dispersion. Nano ZnO particles and ethanol of Merck Limited were used in this study. The nanoparticle of metal oxide (ZnO) was mixed with ethanol and stirred at 60°C for 4 h. This prepared suspension was used for functionalizing the webs via electrospraying process. Optimized web surface of 0.43 g m^{-2} is functionalized by electrospraying technique under identical parameters except voltage is lowered down to 50 kV. Overall, experimental process and techniques are presented in Figure 1, as a flow diagram.

ACS-laminated adsorbent layer. ACS adhered composite fabric is comprised of activated carbon loading of 180 and 210 g m^{-2} and its different components are represented in Figure 2. The technique for making such fabric is known as continuous coating and lamination process. In this process, blended fabric of polyester/viscose is printed with adhesive

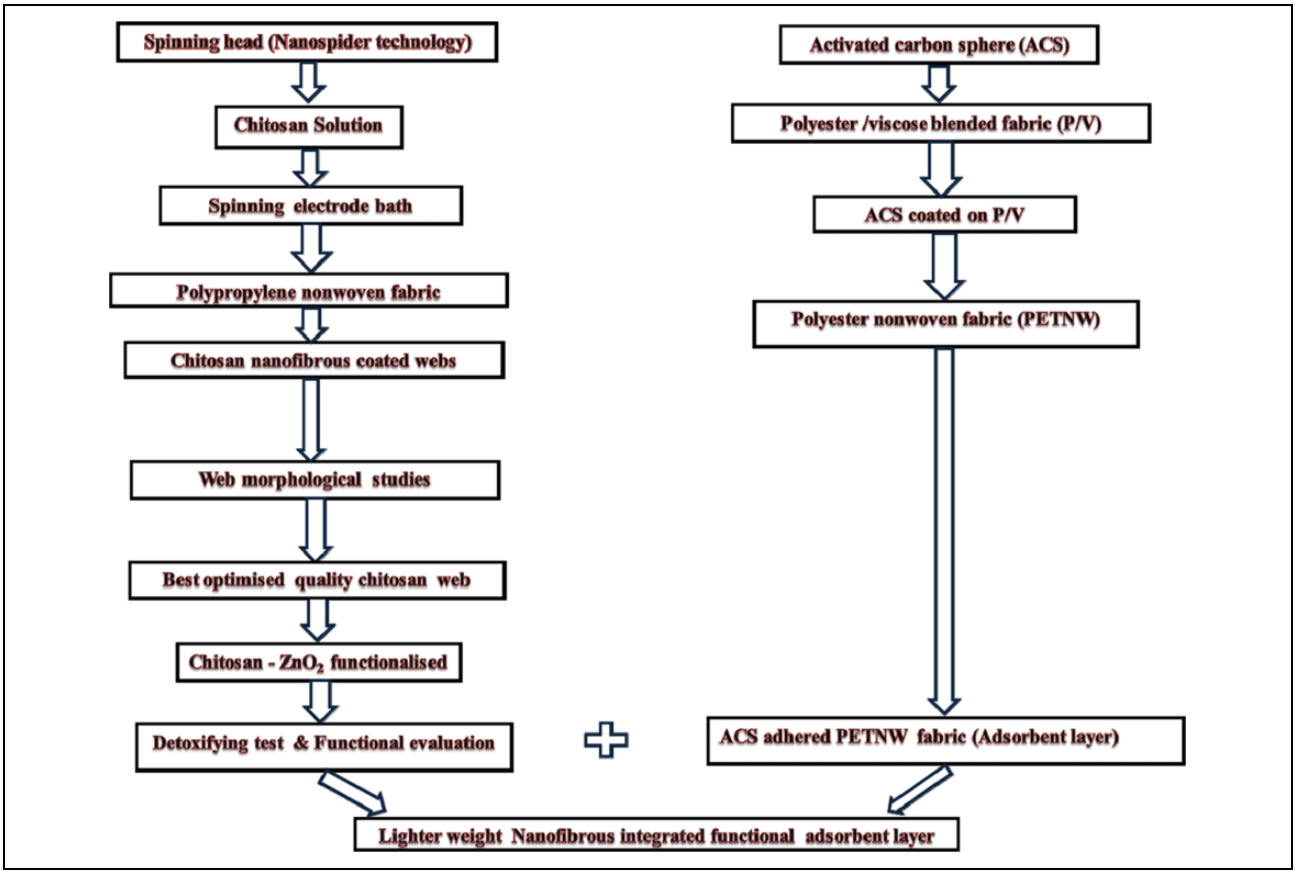

Figure 1. Overall schematic representation of experimental flow diagram.

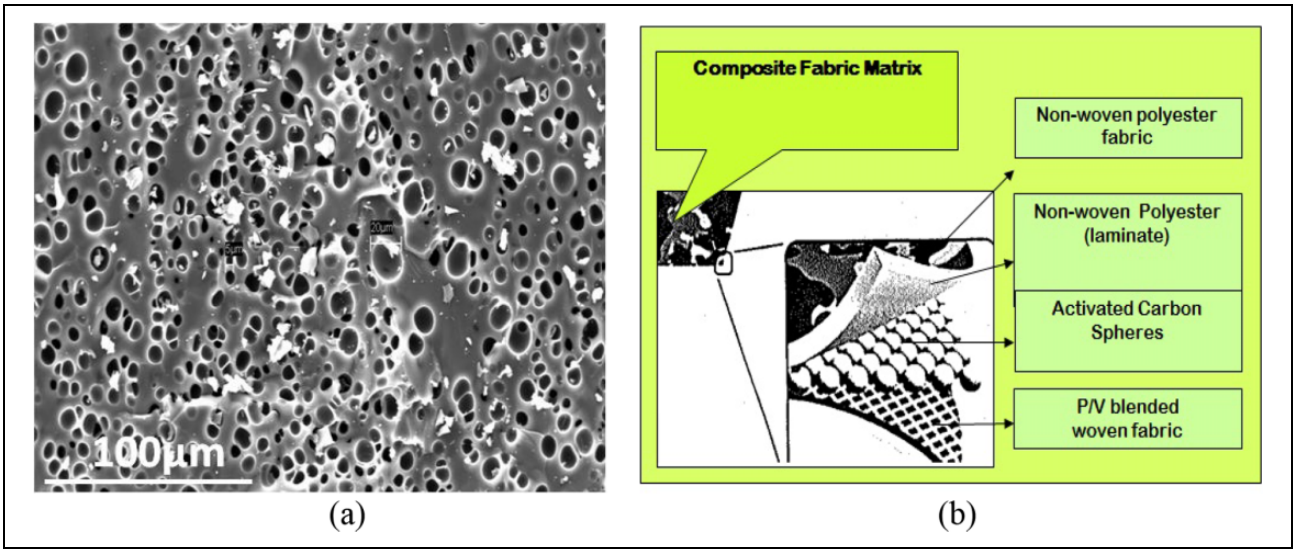

Figure 2. Representative images of (a) porous ACS and (b) different layers in ACS-adhered composite fabric. ACS: activated carbon sphere.

dots and then ACS is dropped onto the fabric through a suitable hopper and mesh arrangements. The ACS deposited on the fabric was cured and fixed at 160–170°C and subsequently, laminated with non-woven fabric by hot roll pressing. The functionalized nanoweb (0.43 g m^{-2}) coated on PP non-woven fabric was stitched with ACS adhered composite fabric for preparation of multilayered fabric structure for evaluation of functional properties: air permeability, biological filtration, antimicrobial and chemical protection.

Surface morphology and diameter. Carl Zeiss EV 050 field emission scanning electron microscopy (FESEM) was used for examining morphology of nanowebs and their images at different scanned areas were captured. Diameters of nanofibres were measured by Image J software (Fiji, Version IJ 1.46r) using the captured images. Forty measurements of random fibres were considered for estimation of average fibre diameter. Density and evenness of the nanowebs were indirectly assessed from visual appearance. The surface of nanofibrous web was also investigated by atomic force microscope (AFM; Agilent 5500 SPM AFM (Agilent Technologies, Inc. W. Arizona, U.S.A.)).

Bacterial filtration. Nanoweb incorporated that PP non-woven fabric and multilayered fabric were clamped between a six-stage cascade impactor and an aerosol chamber at a distance of 15 cm. Bacterial (*Staphylococcus aureus* – ATCC6538) aerosol was generated in chamber using 10 micron nebulizer assembly. The aerosol was drawn through test material using a vacuum attached to cascade impactor. The ratio of upstream to downstream bacterial aerosol count was reported as percentage bacterial filtration efficiency (%BFE).

DCP penetration test. DCP penetration test of nanoweb incorporated that PP non-woven fabric and multilayered fabric were measured using a flame ionization detector unit according to specification no. UK/SC/3346G. The results were recorded in terms of time (seconds) taken to pass vapour of 1 μg min^{-1} of 1,3-DCP through fabric and mean value of five readings was presented.[15]

Air permeability. Air permeability of fabric is defined as volume flow rate per unit area, at a specified pressure differential across the two faces of it. Air permeability of nanoweb-coated non-woven fabric and multilayered fabric was tested on TEXTEST FX 3300 air permeability tester in accordance with ASTM D737 standard.

Water vapour transmission. Breathability (comfort) of adsorbent layer is evaluated in accordance with ASTM E 96, Procedure B (upright cup method). Adsorbent fabrics are placed with coated side facing the water in cup and placed under conditioning chamber 12 $\pm$ 1°C (50% relative humidity) for overnight. The water vapour transmission rate (WVTR) is calculated using the following formula $G/t/A$, where G is weight change (g), t is time during which G occurred and A is test area (m^2) expressed in gram per square meter per 24 h.

Detoxifying test. Best web, which is fulfilling and balancing the properties like breathability, comfort and properties requirements of functionality (DCP test), was chosen for studying its decontamination/self-detoxifying properties. Web is spotted with 10 μl of sulphur mustard gas (HD) and tests like images, Raman spectra, and so on were taken immediately with up most care.

Capillary liquid expulsion porometry. Pore size measurements are made with the Model POROMETER 3G win 10.10 Series automated capillary flow porometer manufactured by Quantachrome Instruments, Inc. Pore sizes are measured by saturating the porous material with a wetting soap liquid.

Antibacterial test. Antibacterial activities of the electrospun nanofibres and fabric were determined by subjecting the membranes into agar plate containing *Escherichia coli* (gram negative) and *S. aureus* (gram positive) and then incubated at 37°C for 24 h. Percentage of reduction in bacterial colonies was determined after 24 h, as per standard test method AATCC 100–2012.

Thermal analysis. Thermogravimetric analysis (TGA; Universal V47A TA) is employed to monitor the changes, which occurred during heating of web under nitrogen (N_2) atmosphere with a heating rate of 10°C min^{-1} with a temperature range between 30°C and 900°C.The obtained TGA curves are interpreted for the thermal behaviour of the samples by matching the endothermic peaks. Moreover, TGA experiments are performed under identical conditions of pyrolization.

Differential scanning calorimetry (DSC; Q 200 V24.8) is used to measure the physical properties of samples under N_2 atmosphere with a heating rate of 10°C min^{-1} in a temperature range between 30°C and 300°C.

Crystalline structure. Wide-angle X-ray diffraction (XRD) traces of webs are recorded with a Phillips diffractometer using copper K_α radiation in reflectance mode (40 kV/20 mA) at a scanning speed of 2 s/0.02°. The samples are scanned from 10° to 80°.

Chemical analysis. Raman spectroscopy is a non-destructive technique, which can be used to characterize Multiwall Carbon Nanotubes (MWCNT) and its interaction with Polyacrylonitrile (PAN) and natural bio-polymeric materials. It is a sophisticated method even to detect the presented elements especially in the nano-level and to investigate the state of carbon. Raman spectroscopy of web is recorded on a Raman and Micro PL system. The spectra over the range 4000–250 cm^{-1} are recorded.

Results and discussion

Morphology of nanowebs

The influence of surface morphology on coated web properties was studied by analysing the measured fibre pore size, DCP, comfort parameters and FESEM images (web's density) by varying collector speed. During spinning of webs, collector speed was varied and, thereby, morphology in terms of between fibre porosity was significantly changed. This mesh morphology ultimately impacts on functional properties of webs. The measured pore size, comfort parameters and FESEM images are presented in Table 1 and Figure 3, respectively.

Table 1. Effect of web morphology on comfort and chemical protective behaviour.

Sample	Coating density (g m^{-2})	Mean pore size (μm)	%BFE	Mean air permeability (cc cm^{-2} s^{-1})	WVTR (g m^{-2}/24 h)	DCP (s)
a	0.04	23.8	39.22	69.6	700.50	90
b	0.07	18.1	44.30	48.6	667.90	101
c	0.13	12.5	63.82	38.2	660.80	105
d	0.22	11.2	86.80	35.5	650.56	115
e	0.43	9.8	91.26	33.6	633.76	145
f	0.61	7.1	93.86	17.4	620.80	155
g	1.01	1.05	97.78	9.5	610.65	165
h	1.25	1.29	96.78	10.6	600.82	180

%BFE: percentage bacterial filtration efficiency; WVTR: water vapour transmission rate; DCP: dichloropropane.

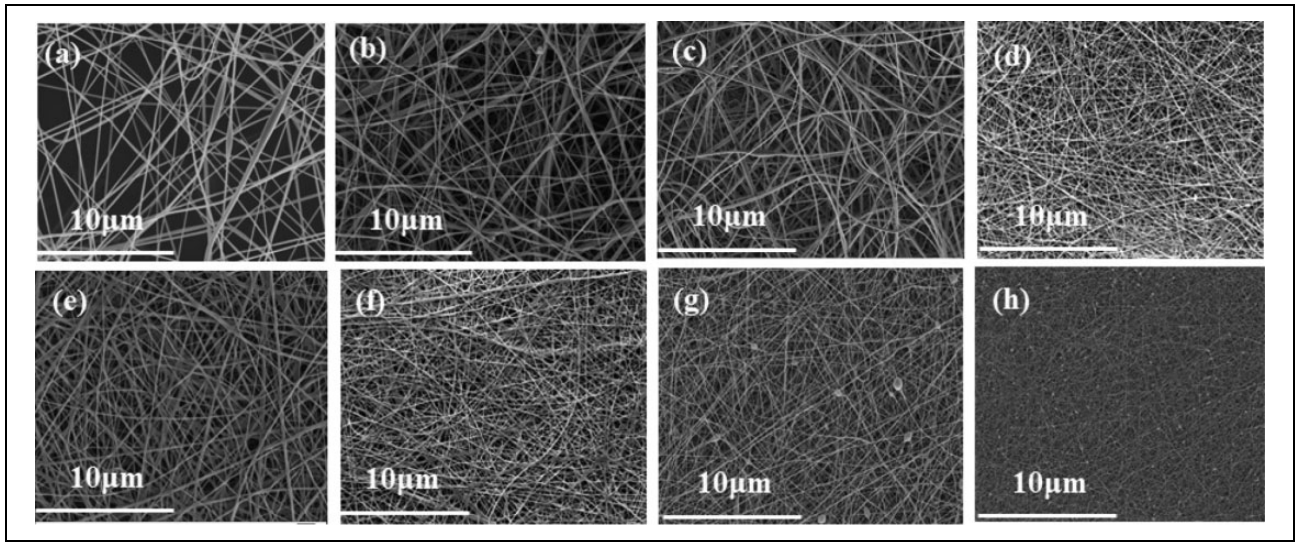

Figure 3. FESEM images of various morphological structure of chitosan webs. FESEM: field emission scanning electron microscopy.

Figure 3(a) to (h) shows a coarser to finer web density of chitosan coated uniformly on PP non-woven fabric. Although it is tedious to electrospin and controlling its morphology due its high polarity and gelling behaviour, a vigorous trail and optimization was conducted with influencing parameters like voltage, electrode distance, spinning electrode speed and solution concentration.[16] A very good morphological structure from chitosan materials was obtained that can be seen from Figure 3(a) to (h). These webs are electrospun and coated under identical process parameters except variation in collector speed, which was resulted in comparable diameter for all samples ranges between approximately 700 nm and 715 nm. Not much difference in the diameter of webs was observed and that was our intention of research. So that comparison could be made with almost identical diameters having different coating densities, which is creating various pattering and layering (morphology) of webs.

It can be seen from Figure 3 and Table 1 that morphology of fibre influenced the properties of chemical barrier as well as comfort level. A reverse trend in comfort, which is measured in terms of air permeability and WVTR, is observed with respect to functional behaviours (DCP) of webs. It is evident that coarser morphology (web density) has better impact on DCP as coated to thinner web. However, at the same time, comfort properties are decreased. Thus, a judicious selection has been made between comfort and functional behaviours based on findings (Table 1 and Figure 2) and standard requirements for existing NBC adsorbent layer (air permeability > 30 cc cm^{-2} s^{-1}, DCP time $= 120$ s and WVTR > 600). Considering these facts, most suitable optimized morphology of coated web was shown in Figure 3(e) (0.43 g m^{-2}), which is taken for further study and integrations with NBC low add-on ACS adhered adsorbent fabric. So that, weight of the overall absorbent could be reduced from the current approximate value of 400–450 g m^{-2}. Tabulated results are well correlated with depicted morphology in Figure 3(a) to (h).

HD spotting test

After selecting the best functional coated webs in terms of functionality and comfort level, it is essential to establish

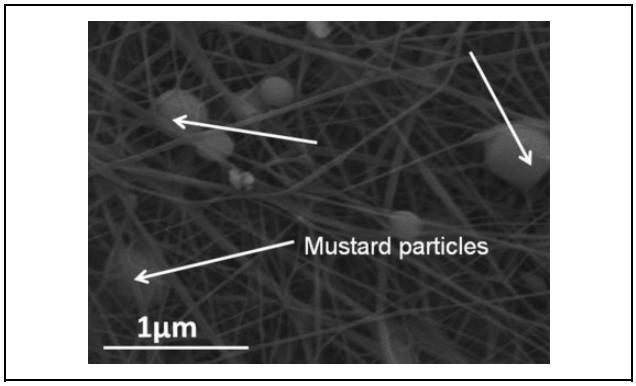

Figure 4. FESEM image of trapped mustard agent (HD) particles. FESEM: field emission scanning electron microscopy.

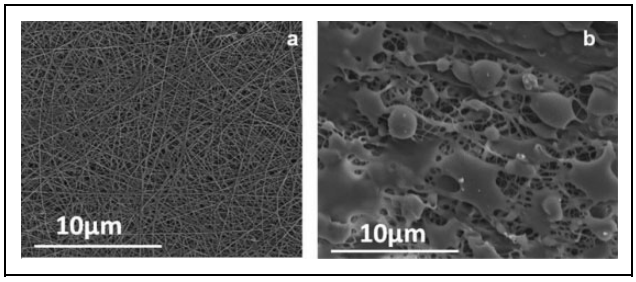

Figure 5. FESEM image of chitosan nanowebs. (a) Non-sprayed. (b) Electrosprayed. FESEM: field emission scanning electron microscopy.

mechanism by which functionality of chemical protection is achieved. Therefore, best optimized web sample was spotted with mustard agent (HD) and it was seen in Figure 4 that web is holding the HD particles and acting as a barrier layer for HD. Moreover, this layer acting as a semi-permeable membrane, where it allows passing water vapour and air and at the same times does not allow penetrating HD chemical particles. However, these HD particles should be detoxified before reuse to avoid any harm to the skin. Hence, the web is functionalized with self-decontaminating agent, namely with ZnO dispersion.

Functionalized web studies

Optimized nanoweb (0.43 g m^{-2}) was eletrosprayed with ZnO dispersion for disintegrating the harmful molecules of HD. It can be seen from Figure 5(b) that relatively homogeneous thick deposition of ZnO appears on the chitosan nanoweb, which is also confirmed by AFM and EDX in Figures 6 and 7, respectively. Energy dispersive X-Ray (EDX) spectrum shows the presence of Zn particles on the web surface.

Thermal analysis

In order to monitor the changes due to heat with respect to as-spun, functionalized and functionalized web spotted

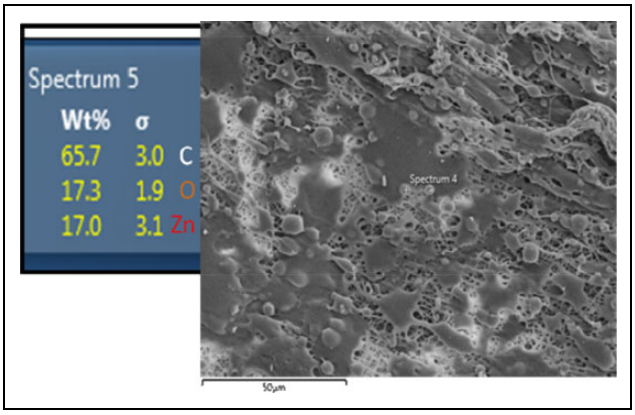

Figure 6. EDX of electrosprayed web of chitosan.

with HD particles, TGA and DSC were employed. Figure 8(a) to (c) shows the TGA traces and some interesting findings were observed. As-spun (Figure 8(a)) shows two stages in weight losses and majority of weight loss of approximately 70.41% in the first stage and approximately 21.66% (800°C) in the second stage, respectively. Majority of decomposition has taken place in the first stage. This signifies that as-spun chitosan has very limited thermal stability. The first stage weight loss was approximately 70.41% in the range of 395–460°C, which might be due to scission of the ether and –OH linkage in the chitosan backbone. In the second stage, the weight losses were approximately 21% in the range of 460–800°C, which relates to the thermal decomposition of inorganic residues. However, a minimal weight loss of approximately 1.47% was seen from 40°C to 395°C and afterwards exothermic phenomenon (+ 0.48%) was observed in functionalized web (Figure 8(b)). This could be due to absorption of heat by Zn particles and its chemical components, which is released as an exothermic phenomenon. Therefore, the functionalized web has shown excellent thermal stability even up to 900°C. At the same time, Figure 8(c), functionalized HD web, shows decomposition in two stages and one exothermic characterizes (first stage of exothermic characterizes with weight loss around + 5.24%). This (2^{nd} stage of decomposition) confirms that after spotting, there is formation of degraded compounds, which is thermally not stable and that appears as higher weight losses approximately 81.44% as compared to minimal weight loss showed by functionalized web. Even, a functionalized web has shown minimal exothermic reactions and, at the same time, exothermic reactions have been increased to +5.24% in HD spotted web. It is certain that reaction has taken place between HD and ZnO. Such vast thermal profile changes have been noticed between functionalized and functionalized HD spotted webs. At this stage, it is very difficult to speculate exact composition of degraded products. Hence, functionalized web shows higher degree of thermal stability as compared to the as-spun webs. We could conclude that TGA thermal profile of as-spun and functionalized HD

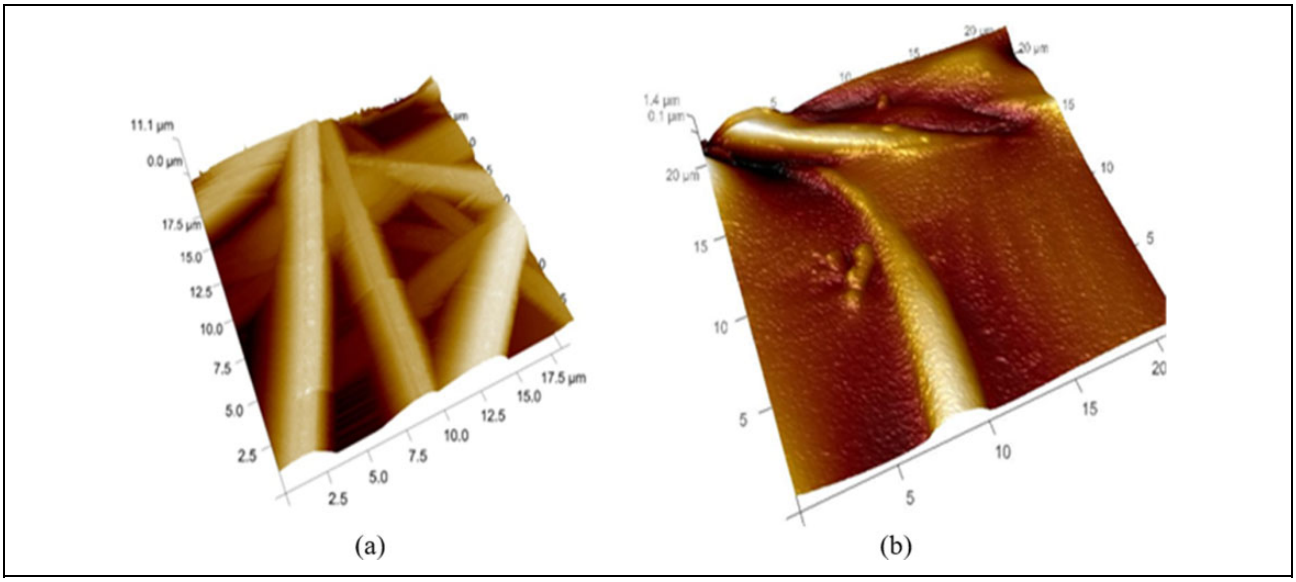

Figure 7. AFM images of chitosan nanowebs. (a) Non-electrosprayed and (b) electrosprayed.

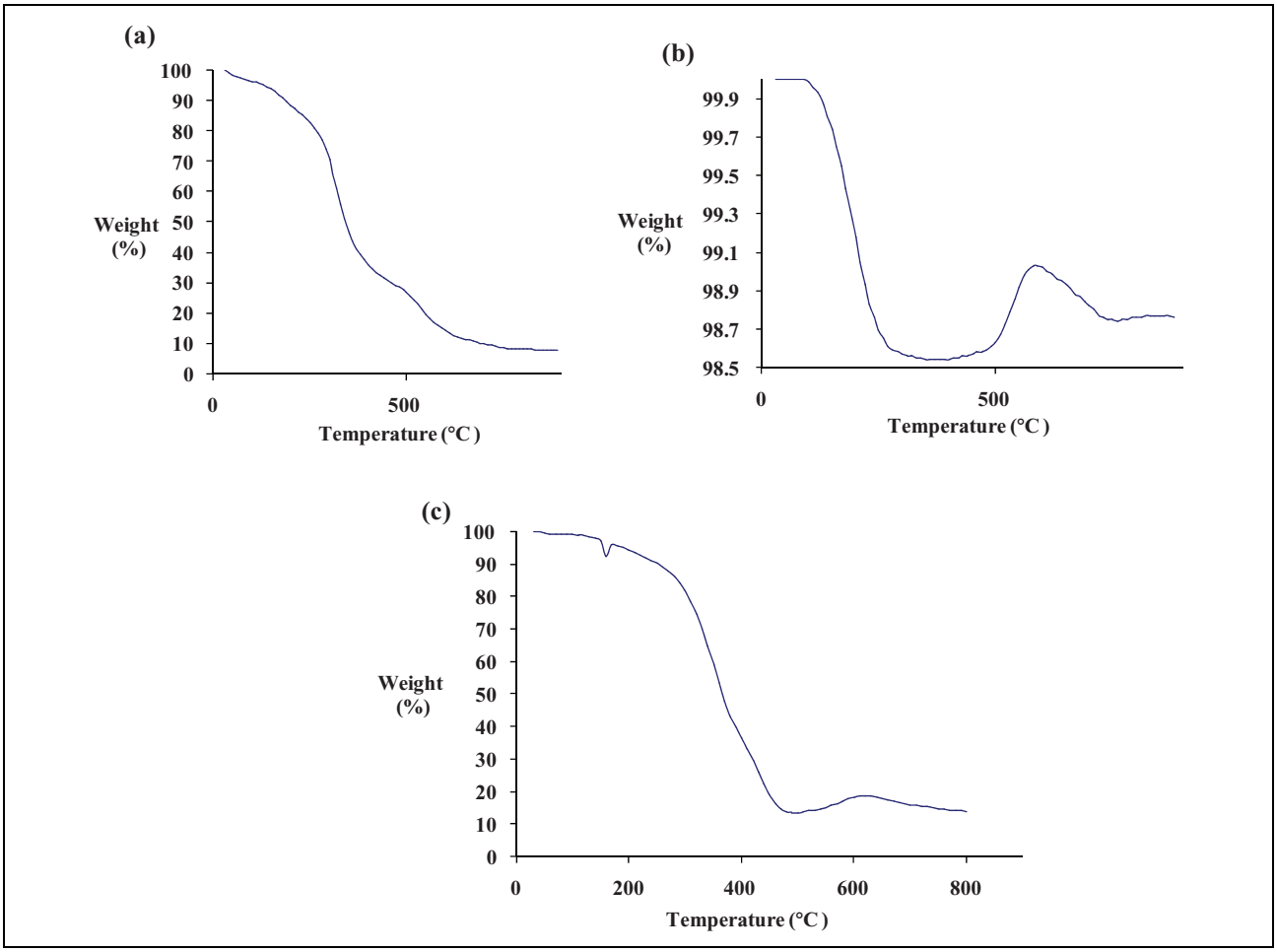

Figure 8. TGA traces of chitosan nanowebs. (a) As-spun, (b) functionalized and (c) HD spotted. TGA: thermogravimetric analysis.

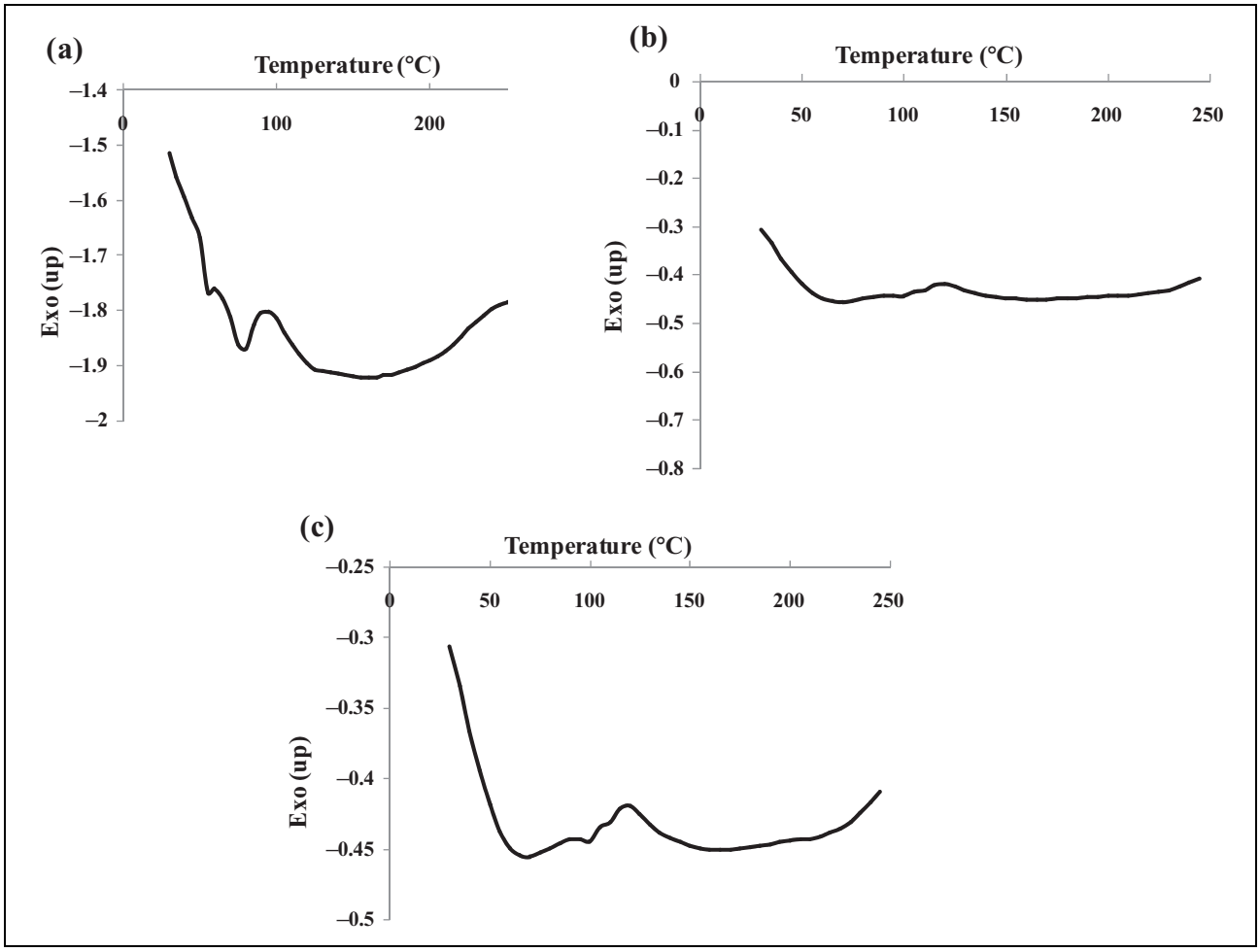

Figure 9. DSC plots of various chitosan nanowebs. DSC: differential scanning calorimetry.

spotted more or less similar. Therefore, it signifies that functionalization is playing a vital role to obtain similar to as spun web even after spotting with HD.

Figure 9(a) to (c) represents the DSC profile of as-spun, functionalized and functionalized web spotted with HD particles, respectively. It can be seen that as-spun web shows endothermic peak around 75°C, which corresponds glass transition (T_g) of chitosan and comparable with other reported results.[17,18] Figure 8(b) shows the same type of thermographs for functionalized web but T_g is not more prominent, as in the case of electrosprayed compounds, which is masking T_g. On the other hand, Figure 8(c) shows T_g identical to as-spun web but peak is board and diffused. This means that some oligomer formation was taken place and resulting in T_g appeared to be diffused and board as compared to as-spun web. HD spotted web also showed exothermic peak around 120°C, which was not appeared in any of two traces. This reveals that there is a formation of some chemical species, which is releasing heat around 120°C. The results obtained by TGA and DSC are agreeable to each other and confirm the disintegration of HD. Hence, the thermal profile gets completely changed for spotted web, as compared to other two traces.

Crystalline structure

XRD plots are shown in Figure 10 and it is evident from the image that as-spun chitosan web shows a board trough around 2θ value of 16.75°, which confirms the presence of amorphous region in the chitosan polymer. But at the same time, a very clear crystalline peak around 2θ value of 25.57° confirms the presence of crystallinity in chitosan. Therefore, it is understood that crystalline structure exists because of presence of –OH and $–NH_2$ groups in the chitosan structure. This result is comparable and in agreement with other researcher.[19] Two small diffused peaks around 2θ value of 44.42° and 54.17° were found in as-spun web. This peak may be due to acetylation or $–NH_2$ products. Moreover, a diffused peak at 2θ value of 21.72° was found in functionalized web and this is possibly due to electrospraying of ZnO which is masking the actual structure of chitosan. Hence, the expected peaks were not visualized. However, HD spotted web showed three board sharp peaks

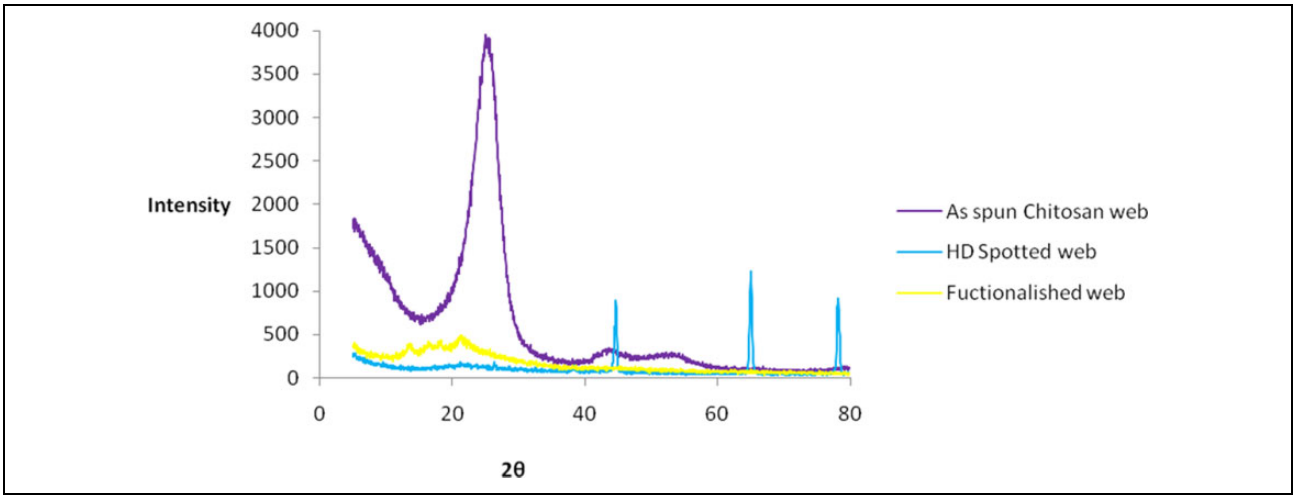

Figure 10. XRD patterns of various chitosan nanowebs. XRD: X-ray diffraction.

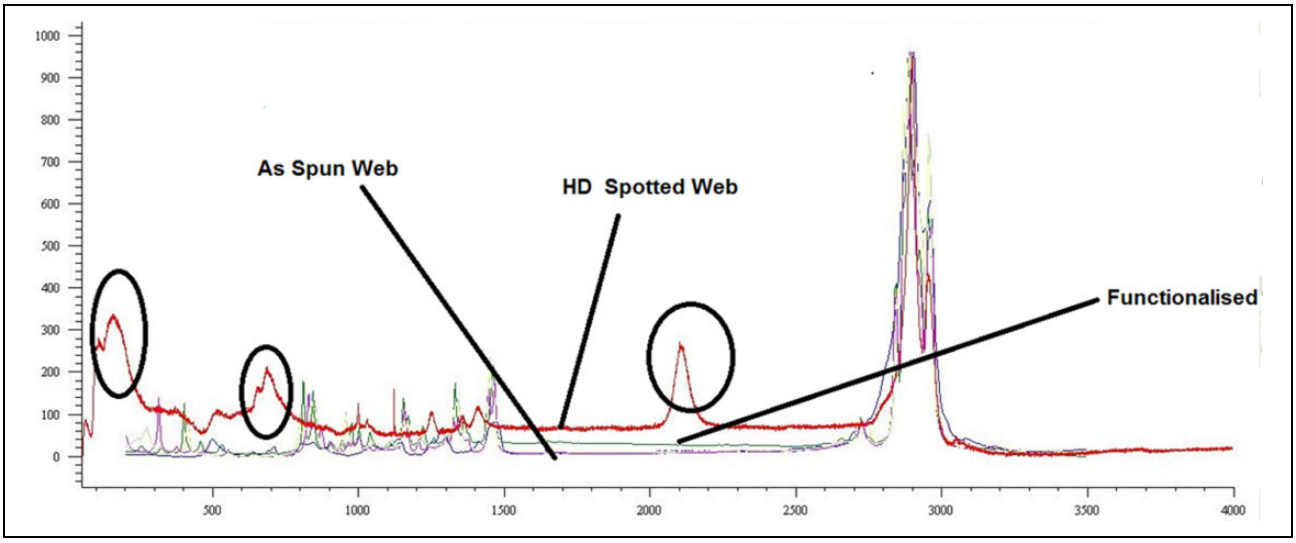

Figure 11. Raman spectra of various chitosan nanowebs.

around 2θ value of 44.72°, 65.02° and 78.22°, respectively. These sharp peaks were not seen in case of other two nanowebs. Therefore, some sort of crystalline structural changes has been developed due to reaction between HD and electrospayed chemical ZnO. Hence, more or less crystalline structural changes have been occurred, which were also confirmed from the DSC and TGA plot's analysis.

Chemical analysis

Now from the above analysis, it is confirmed that structural changes were occurred in the HD spotted webs. However, it is necessary to explore the nature of exact structural changes occurred (physical or chemical). Raman spectroscopy is the best tool/technique to know about functional groups in order to observe any chemical or functional groups changed that has been occurred due to functionalization of nanoweb. The web sample was carefully cut and mounted on the sample holder for the measurement. In case of testing HD spotted webs precautions, including the use of gloves, goggle and safety cabinets were used and immediately withdrawn samples after capturing the traces. Raman spectra plots of webs are shown in Figure 11. Raman spectra of as-spun specimens revealed the strongest peak at 2900 cm^{-1}, arose from $–CH_2$ groups stretching. These peaks appeared in all the three samples. This reported that Raman spectrum for chitosan is comparable with other researchers.[20–22] But HD spotted web showed a sharp peak around 700 cm^{-1}, which might be due to presence of sulphur compounds, which is also reported elsewhere.[21,22] In the same web, we observed a new peak around 2100 cm^{-1}. This confirmed the formation of new –OH functional group containing compounds, which was not appeared in other two Raman traces. Thus, the data exhibit the formation of non-toxic hydrolysis products in the

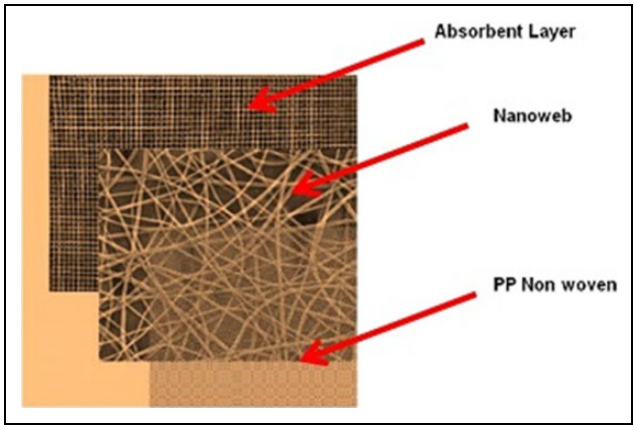

Figure 12. Schematic diagram of integration web with NBC adsorbent layer. NBC: nuclear, biological and chemical.

detoxification of HD, by functionalized nanoweb (ZnO), spotted with HD. This might be due to formation and combination of two –OH (hydroxyl) free radical species combing together to produce hydrogen peroxide, which is destroying and disintegrating HD molecules.

Web integration and functional behaviours

Integration of nanowebs with fabrics for applications other than DPTs was reported elsewhere.[1,2,23–26] Considering this fact, such concept of integration of nanoweb layer into DPTs is evolved for creating DPT fabrics of (a) lower weight, (b) elimination of bulky layered structure from DPTs, (c) better comfort and (d) improved functionalities by integrating. It was proven that functionalized nanoweb was detoxified by breaking the molecules of HD and also working as a barrier agent with adequate level of comfort. After getting such encouraging findings, then subsequently, nanoweb (0.43 g m^{-2}) was integrated with ACS fabric with ACS add-on of 180 and 210 g m^{-2} to observe functional behaviours. The intention of integration is to reduce the weight of NBC suit by adding nanofibrous layers. It was observed that alone nanoweb layer is not fulfilling all these functional requirements and also not able to withstand rugged soldiers combat operations. A schematic diagram of integration is shown in Figure 12. The measured values of BFE and air permeability and DCP of multilayered fabrics are shown in Table 2.

The optimized coating density was selected for stitching with ACS-adhered composite fabric for evaluation of chemical protection, %BFE, DCP penetration rate (seconds) and comfort level and the results are presented in Table 2. It was evident that chemical protection was increased very significantly from 105 s to 270 s. The increase of chemical protection is due to presence of large number of very small size of pores in the nanoweb, as evident from Table 1 and FESEM images. ACS fabric has shown very poor bacterial filtration properties. Moreover, by adding nanofibre layer, biological filtration has

Table 2. Assessment of biological and chemical protection.

Sample number	Description	%BFE	Air permeability (cc cm^{-2} s^{-1})	WVTR (g m^{-2}/ 24 h)	DCP (s)
1	ACS add-on 180 g m^{-2}	10.01	31.26	551.10	105
2	ACS add-on 210 g m^{-2}	15.21	22.5	450.21	170
3	Multilayered fabric ACS add-on 180 g m^{-2}	93.02	32.1	610.56	270
4	Multilayered fabric ACS add-on 210 g m^{-2}	93.47	26.5	555.56	295

%BFE: percentage bacterial filtration efficiency; WVTR: water vapour transmission rate; DCP: dichloropropane; ACS: activated carbon sphere.

Table 3. Evaluation of antimicrobial protective behaviour of webs and fabrics.

Sample number	Description	*Staphylococcus aureus* ATCC 6538	*Escherichia coli* ATCC 25922
		% Reduction	% Reduction
1	Base coating substrate fabric (PP)	No reduction	No reduction
2	Nanoweb-coated layer 0.43 g m^{-2}	96.65	91.93
3	ACS add-on 180 g m^{-2}	No reduction	No reduction
4	Multilayered fabric (nano web + ACS add-on 180 g m^{-2})	99.96	99.25

PP: polypropylene; ACS: activated carbon sphere.

increased significantly. Hence, it can be concluded that nanofibre layer is producing additional functional features of biological protection, which was not found earlier in ACS fabric used for NBC suit. It was noticed that %BFE increased and air permeability decreased with increasing in coating density of nanowebs, as observed from Table 1. As both the parameters are contradictory in nature, the optimized combination of both can be selected to meet clothing requirements. Hence, coating density of 0.43 g m^{-2} can be treated as optimized coating, as it is offering %BFE = 91.26 with air permeability of 33.6 cc cm^{-2} s^{-1}. Air permeability of 30.0 cc cm^{-2} s^{-1} is considered as minimum value for offering clothing comfort. The selected coating density in combination with ACS adhered multilayered fabric is also offering %BFE = 93.02 with air permeability of 32.1 cc cm^{-2} s^{-1} at lower ACS add-on of 180 g m^{-2}. However, higher ACS add-on (210 g m^{-2}) does not fulfil comfort properties but offering enhanced chemical protection of DCP time = 225 s. This means that nanofibre

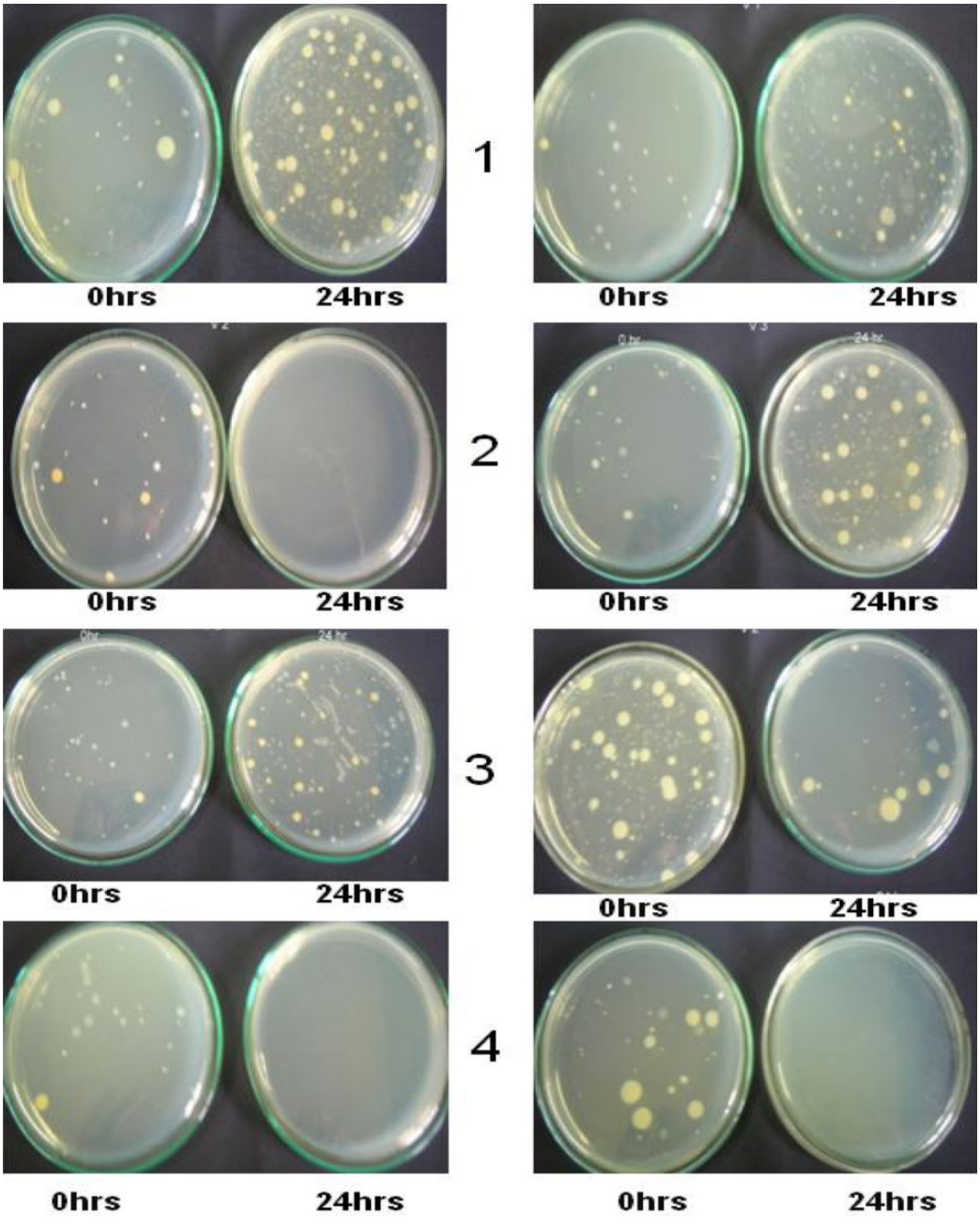

Figure 13. Agar plate images. Left: *Staphylococcus aureus* (gram positive) and right: *Escherichia coli* (gram negative) showing bacterial incubation after 24 h of (1) non-woven PP, (2) nanoweb-coated layer, (3) ACS-laminated fabric and (4) multilayered ACS fabric, respectively. PP: polypropylene; ACS: activated carbon sphere.

layer is governing and controlling the comfort properties (interlinked small and large number pores) but as we go to higher ACS add-on, packing density impacts on the clothing comfort.

Antimicrobial properties

Table 3 and Figure 13 provide the antimicrobial activity of nanowebs and adsorbent layers after 24 h of bacterial incubation. It can be noticed that multilayered fabric (ACS-laminated fabric + chitosan nanoweb) has provided more than approximately 99% of bacterial reduction after 24 h. It is also seen that after nanoweb coating on PP non-woven fabric, approximately 92% reduction in bacterial colonies was observed against both kind of bacteria. However, base substrate (PP non-woven fabric) and ACS-laminated fabric alone do not show any reduction in bacterial colonies. This signified that chitosan material is

playing a complete role in controlling microbial protective behaviour of fabrics.[27] This bacterial reduction is due to inherent chemical nature of chitosan polymer. Chitosan material is having hydroxyl (–OH) and amino groups (–NH_2) in the back bone of chain. These chemical species dissociate and attaching/arresting chemical species (positive ions and negative ions) present in the bacterial colonies and thereby causes destroying activity of bacteria. The results expressed in % reduction are well correlated with showed agar plate colonies, as depicted after 24 h of bacterial incubation (Figure 13).

Conclusions

In this research work, protective action has been achieved by two theories: (1) barrier and trapping of HD and (2) disintegration of HD may be due to free radical hydrolysis mechanism. AFM and EDX confirm the presence of Zn particles on functionalized web. Raman spectra plots confirm the formation of new chemical product at 2100 cm^{-1} due to functionalization. The obtained Raman results of structural changes in functionalized HD spotted web are well correlated with XRD, TGA and DSC[28] analysis.

This research initiative successfully established that with minimum weight addition of nanoweb-coated nonwoven fabric (approximately 30.43 g m^{-2}), there is a significant improvement in biological and chemical protection of ACS adhered composite fabric. The optimized coating density is decided to be 0.43 g m^{-2} for offering biological protection (%BFE = approximately 92) with maintaining clothing comfort. Chemical protection was increased significantly with offering DCP penetration time of 270 s and this empirically contributes chemical protection of 40 h. Hence, the futuristic NBC suit can consist of such combination of ACS-adhered composite fabric or activated carbon fabric with nanofibrous web to offer biological protection with much higher level of chemical protection. This study has showed optimized nanofibrous web coating density with new morphology, improved air and water transportation permeability (comfort), with offering adequate chemical protection and additionally, incorporated biological and antimicrobial features under single umbrella for DPTs. In short, nanofibre web is acting as a semipermeable membrane, which allows passing water vapour and air but does not allow passing CWA (HD). An additional feature of antimicrobial activity has been shown by both bacteria (*S. aureus* (gram positive) and *E. coli* (gram negative)) and % reduction in the range of approximately 99% after incubation 24 h.

Such lightweight multilayered fabric could be considered as a multifunctional fabric with various functional features and highly beneficial to DPTs. Further work is required to carry out in order to increase its adhesion properties with coating substrate, useable fastness properties and durability. Continual research work is going on to laminate and increase its durability. Such that, these webs will be suitable for rugged combat and repeated wash fastness and these materials will be treated as the strong candidate for the development of next generation lightweight NBC suit for Indian soldiers.

Acknowledgement

The authors are thankful to Dr N. Eswara Prasad, Director, DMSRDE, Kanpur, for his constant support guidance in carrying out this research work and continuous encouragement for making necessary corrections.

Declaration of conflicting interests

The author(s) declared no potential conflicts of interest with respect to the research, authorship, and/or publication of this article.

Funding

The author(s) received no financial support for the research, authorship, and/or publication of this article.

References

1. Bagherzadeh R, Latifi M, Najar SS, et al. Transport properties of multilayer fabric based on electrospun nanofiber mats as a breathable barrier textile material. *J Text Res* 2012; **82**(1): 70–76.
2. Ramkumar SS, Love AH, Sata UR, et al. Next-Generation nonparticulate dry nonwoven pad for chemical warfare agent decontamination. *Ind Eng Chem Res* 2008; **47**(24): 9889–9895.
3. Lu P and Ding B. Applications of electrospun fibers. *Recent Pat Nanotechnol* 2008; **2**(3): 169–182.
4. Chen JP, Chen SH and Lai GJ. Preparation and characterization of biomimetic silk fibroin/chitosan composite nanofibers by electrospinning for osteoblasts culture Nanoscale. *Res Lett* 2012; **7**(1): 170–181.
5. Nasreen SA, Sundarrajan S, Nizar SA, et al. Advancement in electrospun nanofibrous membranes modification and their application in water treatment. *Membranes (Basel)* 2013; **3**(4): 266–228.
6. Faccini M, Vaquero C and Amantia D. Development of protective clothing against nanoparticle based on electrospun nanofibres. *J Nanomater* 2012; **12**: 1–9.
7. Jeong SI, Krebs MD, Bonino CA, et al. Electrospun chitosan–alginate nanofibers with in situ polyelectrolyte complexation for use as tissue engineering scaffolds. *Tissue Eng Part A* 2011; **17**(1–2): 59–70.
8. Shih-Jung L, Yi-Chuan K, Chi-Yin C, et al. Electrospun PLGA/collagen nanofibrous membrane as early-stage wound dressing. *J Memb Sci* 2010; **355**: 53–59
9. Zhang S, Woo SS and Kim J. Design of ultra-fine nonwovens via electrospinning of Nylon 6: Spinning parameters and filtration efficiency. *Mater Design* 2009; **30**(9): 3659–3666.
10. Martinova L and Lubasova D. Electrospun chitosan based nanofibres. *Res J Text Apparel* 2008; **12**(2): 72–79.

11. Geng X, Kwon OH and Jang J. Electrospinning of chitosan dissolved in concentrated acetic acid solution. *Biomaterials* 2005; **26**(27): 5427–5432.
12. Ohkawa K, Minato KI, Kumagai GO, et al. Chitosan nanofibre. *Biomacromolecules* 2006; **7**(11): 3291–3294.
13. Pillai CKS and Sharma CP. Electrospinning of chitin and chitosan nanofibres trends Biomater. *Artif Organs* 2009; **22**(3): 179–201.
14. Eichhorn SJ and Sampson WW. Relationships between specific surface area and pore size in electrospun polymer fibre networks. *J Res Soc Interface* 2010; **7**(45): 641–649.
15. Singh B, Suryanarayana MVS, Baronia SM, et al. Evaluation of chemical protective clothing: a comparative study of breakthrough times with sulphur mustard and a simulant, 1, 3 dichloropropane. *Def Sci J* 2000; **50**: 51–57.
16. Jacobs V, Patanaik A and Anandjiwala RD. Electrospun chitosan nanofibre membranes for antimicrobial application: role of electrospinning processing parameters. *Eur Cell Mater* 2010; **19**: 1–4.
17. Dhawade PP and Jagtap RN. Characterization of the glass transition temperature of chitosan and its oligomers by temperature modulated differential scanning calorimetry. *Adv Appl Sci Res* 2012; **3**: 1372–1382.
18. Mostafa AD, El-Sonbati AZ, Al-Halawany MM, et al. Thermal stability and degradation of chitosan modified by cinnamic acid. *Open J Polym Chem* 2012; **2**(1): 14–20.
19. Henych J, Janos P, Kormunda M, et al. Reactive adsorption of toxic organophosphates parathion methyl and DMMP on nanostructured Ti/Ce oxides and their composites. *Arabian J Chem* 2016. DOI: 10.1016/j.arabjc.2016.06.002.
20. Steven C, Brian MA, Lawrence P, et al. Nonintrusive analysis of chemical agent identification sets using a portable fiber-optic Raman spectrometer. *Appl Spectrosc* 1999; **53**: 850–854.
21. Zając A, Hanuza J, Wandas M, et al. Determination of N-acetylation degree in chitosan using Raman spectroscopy. *Spectrochim Acta Part A: Mol Biomol Spectrosc* 2015; **134**: 114–120.
22. Stuart DA, Biggs KB and Van Duyne RP. Surface-enhanced Raman spectroscopy of half-mustard agent. *The Analyst* 2006; **131**(4): 568–572.
23. Shannon JL, Stephen FR, Nicolas M, et al. A novel enzymatic bioelectrode system combining a redox hydrogel with a carbon nanoweb. *Chem Commun* 2011; **47**: 8886–8888.
24. Ding B, Wang M, Wang X, et al. Electrospun nanomaterials for ultrasensitive sensors. *Mater Today* 2010; **13**(11): 16–27.
25. Turaga U, Singh V, Gibson A, et al. Preparation and characterization of bioactive and breathable polyvinyl alcohol nanowebs using a combinational approach. *Nanotechnol* 2016; **15**: 653–660.
26. Huang Q, Liu L, Wang D, et al. One-step electrospinning of carbon nanowebs on metallic textiles for high-capacitance supercapacitor fabrics. *J Mater Chem A* 2016; **18**: 6802–6808.
27. Arkoun M, Daigle F, Heuzey MC, et al. Antibacterial electrospun chitosan-based nanofibers: a bacterial membrane perforator. *Food Sci Nutr* 2017; **5**(4): 865–874.
28. EL-Hefian EA, Elgannodi E, Mainal A, et al. Characterization of chitosan in acetic acid: rheological and thermal studies. *Turk J Chem* 2010; **34**: 47–56.